April 1999 • NREL/CP-520-29589

Conference Paper

Next Generation Thin Films for Photovoltaics: InGaAsN

Preprint

E.D. Jones, A.A. Allerman, J.F. Klem,
S.R. Kurtz, and N.R. Modine
Sandia National Laboratories

D.J. Friedman and J.F. Geisz
National Renewable Energy Laboratory

W. Shan and W. Walukiewicz
Lawrence Berkeley National Laboratories

C. Tu
University of California San Diego

To be presented at the Electrochemical Society International Symposium
Seattle, Washington
May 2-6, 1999

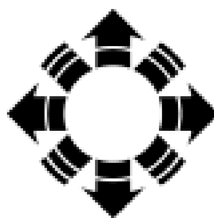

National Renewable Energy Laboratory

1617 Cole Boulevard
Golden, Colorado 80401-3393

NREL is a U.S. Department of Energy Laboratory
Operated by Midwest Research Institute • Battelle • Bechtel

Contract No. DE-AC36-99-GO10337

NOTICE

The submitted manuscript has been offered by an employee of the Midwest Research Institute (MRI), a contractor of the US Government under Contract No. DE-AC36-99GO10337. Accordingly, the US Government and MRI retain a nonexclusive royalty-free license to publish or reproduce the published form of this contribution, or allow others to do so, for US Government purposes.

This report was prepared as an account of work sponsored by an agency of the United States government. Neither the United States government nor any agency thereof, nor any of their employees, makes any warranty, express or implied, or assumes any legal liability or responsibility for the accuracy, completeness, or usefulness of any information, apparatus, product, or process disclosed, or represents that its use would not infringe privately owned rights. Reference herein to any specific commercial product, process, or service by trade name, trademark, manufacturer, or otherwise does not necessarily constitute or imply its endorsement, recommendation, or favoring by the United States government or any agency thereof. The views and opinions of authors expressed herein do not necessarily state or reflect those of the United States government or any agency thereof.

Available electronically at http://www.doe.gov/bridge

Available for a processing fee to U.S. Department of Energy
and its contractors, in paper, from:
U.S. Department of Energy
Office of Scientific and Technical Information
P.O. Box 62
Oak Ridge, TN 37831-0062
phone: 865.576.8401
fax: 865.576.5728
email: reports@adonis.osti.gov

Available for sale to the public, in paper, from:
U.S. Department of Commerce
National Technical Information Service
5285 Port Royal Road
Springfield, VA 22161
phone: 800.553.6847
fax: 703.605.6900
email: orders@ntis.fedworld.gov
online ordering: http://www.ntis.gov/ordering.htm

Printed on paper containing at least 50% wastepaper, including 20% postconsumer waste

NEXT GENERATION THIN FILMS FOR PHOTOVOLTAICS: InGaAsN

E. D. Jones[a], A. A. Allerman[a], D. J. Friedman[b], J. F. Geisz[b], J. F. Klem[a], Steven R. Kurtz[a], N. R. Modine[a], W. Shan[c], C. Tu[d], and W. Walukiewicz[c]

a)Sandia National Laboratories, Albuquerque, NM
b)National Energy Renewable Laboratory, Golden CO
c)Lawrence Berkeley National Laboratories, Berkeley, CA
d)University of California San Diego, La Jolla, CA

A new semiconductor alloy system, InGaAsN, has been identified as a candidate material for multi-junction solar cells having efficiencies greater than 40%. The introduction of small amounts of nitrogen (~2%) into the InGaAs alloy system greatly reduces the band gap energy, with reductions approaching 0.4 eV for 2% nitrogen content! With the appropriate ratio of indium to nitrogen concentrations, InGaAsN can be lattice matched to GaAs.

1. INTRODUCTION

The quaternary alloy system, InGaAsN, is a new material system that appears to have many exciting and important device applications. Because of a large negative bowing parameter,[1,2] the addition of small amount of nitrogen to the 1.4 eV bandgap energy GaAs system *lowers the energy*! In addition to lowering the bandgap energy, adding indium to GaAsN strain compensates the effect of nitrogen, resulting in a material system with bandgap energies ~ 1eV and lattice matched to GaAs! The InGaAsN, alloy system has been identified as a key candidate material for long wavelength laser systems[3-5] and high-efficiency multi-junction solar cells.[6,7] Before the successful realization of multijunction solar cells which utilize thin films of InGaAsN as an integral part, questions regarding the role of the nitrogen isoelectronic atom in GaAs must be addressed. In particular: (1) What is the physical (or chemical) origin of the large bandgap reduction? (2) Are the nitrogen induced states extended (band-like) or localized (impurity-like)? (3) Are the observed low conduction-band mobilities intrinsic to InGaAsN? and (4) Are recombination times between the conduction and valence band states seriously affected?

This paper will address the aforementioned questions by reviewing some of the current experimental and theoretical information for the InGaAsN material system. Section 2 discusses InGaAsN thin film metalorganic chemical vapor deposition (MOCVD) and molecular beam epitaxy (MBE) growth techniques and growth parameters which result in the highest quality films suitable for incorporating into multijunction solar cells. The topic of Section 3 is the measurement minority carrier diffusion lengths. Also discussed in Section 3 are measurements of carrier lifetimes and internal quantum efficiencies. Photomodulated absorption spectroscopy results are discussed in Sec. 4 and an analysis of the data in terms of a simple two level system with anticrossing behavior is shown to give good agreement. Results from first principle band structure calculations using the local density approximation are presented in Sec. 5. Here it is shown that while the calculated value for the bandgap energy is in poor agreement with experiment, the agreement between the experimental and theoretical bandgap energy pressure coefficients is excellent. Section 6 outlines some

key issues that need to be solved before InGaAsN can assume its anticipated role as the next generation thin film material for high efficiency solar cells. Finally, conclusions are presented.

2. THIN FILM GROWTH

MOCVD Growth

Thin (< 0.5 μm) $In_xGa_{1-x}As_{1-y}N_y$ films were grown using trimethylindium (TMIn), trimethylgallium (TMG), 100% arsine and dimethylhydrazine (DMHy). Dimethylhydrazine was used as the nitrogen source since it has a lower disassociation temperature than ammonia and has a vapor pressure of approximately 110 torr at 18°C. It was found that unintentionally doped InGaAsN epilayers are p-type. InGaAsN films for Hall and optical measurements were grown on semi-insulating GaAs orientated 2° off (100) towards <110>. Lattice matched films ($\delta a / a < 8 \times 10^{-4}$)were grown at 600°C and 60 torr using a V/III ratio of 97, a DMHy/V ratio of 0.97 and a TMIn/III ratio of 0.12. The growth rate was 10Å/s. These conditions resulted in films with an indium mole fraction of 0.07 ± 0.005 and a nitrogen mole fraction of 0.022 ± 0.003. The composition was determined by calibration growths of GaAsN and InGaAs along with double crystal x-ray diffraction measurements. The nitrogen composition of bulk films was also confirmed from elastic recoil detection measurements. A significant increase in photoluminescence intensity was observed from these films following a post-growth anneal. Ex-situ, post-growth anneals were carried out in a rapid thermal anneal system under nitrogen using a sacrificial GaAs wafer in close proximity to the InGaAsN sample.Undoped InGaAsN/GaAs strained quantum wells are also of great interest to 1.3 mm vertical-cavity surface-emitting lasers. Incorporation of N in GaInAs, however, is found to quench photoluminescence (PL), but rapid thermal annealing (RTA) can improve the PL intensity.[8] For solar cell applications a 1 - 2 μm thick layer, lattice-matched to the GaAs substrate, with n- and p-type doping is desired.

Nitrogen incorporation on the order of 1% into GaAs has also been accomplished using plasma-cracked NH3,[9] dimethylhydrazine (DMHy)[10] and hydrazine as N sources. By far, the most common nitrogen source currently is dimethylhydrazine due to its easy incorporation into existing MOCVD systems and high vapor pressure.

Typical MOCVD growth of epitaxial $In_xGa_{1-x}As_{1-y}N_y$ layers on GaAs use trimethylindium (TMIn), trimethylgallium (TMG), arsine and dimethylhydrazine (DMHy) as sources. Lattice matched films (δa / a < 8 x10-4) can be grown at 600°C, 60 torr and 10Å/s using a V/III ratio of 97, a DMHy/V ratio of 0.97 and a TMIn/III ratio of 0.12. These conditions result in films with an indium mole fraction of 0.07 ± 0.005 and a nitrogen mole fraction of 0.022 ± 0.003. The composition has been determined by calibration growths of GaAsN and InGaAs along with double crystal x-ray diffraction measurements. The nitrogen composition of bulk films has also been confirmed from elastic recoil detection measurements and secondary ion mass spectroscopy (SIMS). A wide range of other growth conditions have also resulted in lattice-matched InGaAsN films, but the material must be grown at low temperatures and high DMH/V ratios[11] to incorporate sufficient nitrogen. Nitrogen incorporation also appears to be suppressed with increasing In content.[12]

Current challenges in the growth of InGaAsN by MOCVD techniques include high background carrier concentrations, unintentional incorporation of impurities, intentional doping, and low diffusion lengths. The most important issue for solar cell devices is

(a) (b)

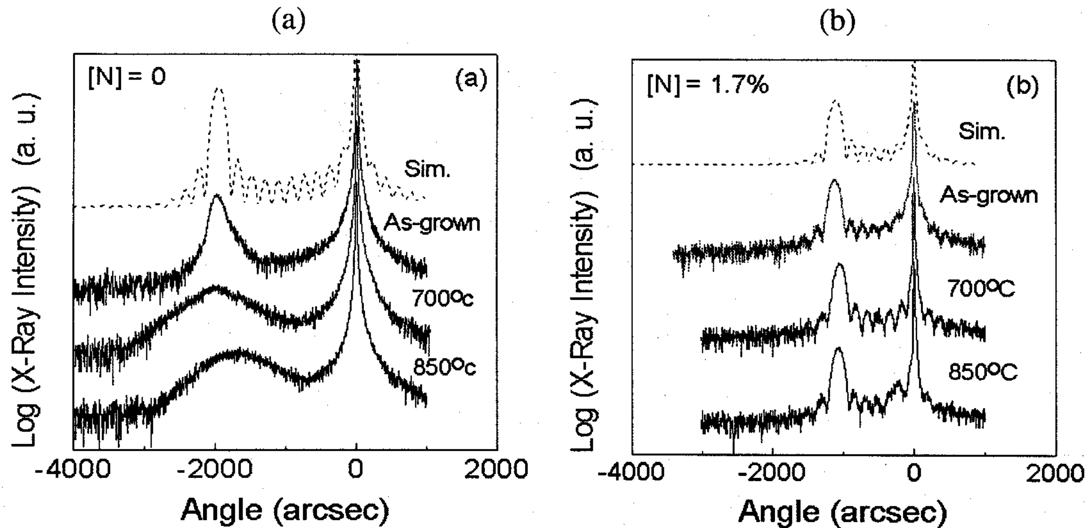

Figure1. X-ray rocking curves of as-grown and annealed $In_{0.108}Ga_{0.892}As$ (Fig. 1(a)) and $In_{0.108}Ga_{0.892}N_{0.017}As_{0.983}$ (Fig. 1(b)) samples, respectively. The dashed lines correspond to simulation results.

minority carrier diffusion lengths. Growth of InGaAsN to date has not yielded any material with sufficiently long diffusion lengths for typical high efficiency III-V structures.[12] The reason for these low diffusion lengths remains unclear. Recent understanding of the band structure of this material explains observed low electron mobilities, but this alone does not completely explain the poor diffusion lengths. Theoretical calculations based on the current understanding of the band structure has not yet been able to predict the intrinsic limits to carrier lifetimes in this material. Direct, reliable measurements of minority carrier lifetimes and diffusion lengths also remain elusive. These topics are discussed in greater detail in Section 3.

Annealing of the material has been shown to improve PL intensities,[8] hole mobilities,[13] and cell characteristics.[14] Reduced deep-level densities by annealing have also been reported.[15] Carrier concentration can also be dramatically affected by annealing.[13] Annealing conditions (e.g. ambient gas, temperature, time) can dramatically affect the results of annealing but these effects are not well understood because the actual microscopic effect of annealing the material is not yet known.

InGaAsN grown by MOCVD on GaAs is typically found to be p-type ~ 1×10^{17} cm^{-3}. High carbon and hydrogen contamination in MOCVD-grown InGaAsN has been observed by SIMS. It has been postulated by many that the p-type background is due to the carbon acceptor partially passivated by hydrogen, but this has not been proven. The role of these unintentional contaminants in terms of potential deep trap centers that reduce diffusion lengths has not been deciphered. Demonstration of hydrogen and carbon free material may help elucidate this question. Intentional p-type doping with C and Zn has proved to be straightforward, but n-type doping remains problematic. The efficiency of Si doping efficiency by disilane is greatly reduced in InGaAsN materials in a temperature dependant manner implying problems with pre-reaction in the gas-phase. Se doping with H_2Se on the other hand is extremely efficient at the low temperature, low arsine pressures typically employed.

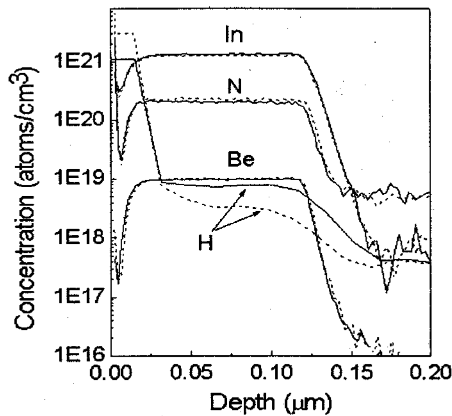

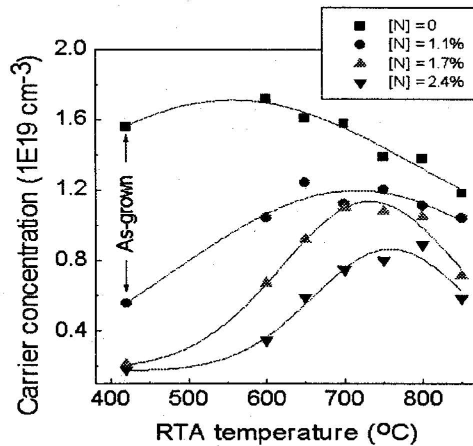

Figure 2. SIMS profiles of as-grown (solid lines) and 700°C-annealed (dashed lines) for the $Ga_{0.892}In_{0.108}N_{0.017}As_{0.983}$ samples.

Figure 3. Free carrier concentrations as a function of RTA temperature for as-grown and annealed InGaAsN samples

MBE Growth

Highly Be-doped p-type ($\sim 1 \times 10^{19}$ cm^{-3}), 110-nm-thick $In_{0.108}Ga_{0.892}N_xAs_{1-x}$ layers on semi-insulating GaAs substrates have been grown[16] by gas-source molecular beam epitaxy with cracked arsine and a RF plasma nitrogen radical beam source. The compositions were determined by X-ray rocking curve (XRC) measurements and simulations based on the dynamical theory. A 10 second RTA was performed on these samples with halogen lamps in a flowing N_2 ambient. During RTA, the samples were put on a GaAs wafer face-to-face to prevent the loss of arsenic at elevated temperatures.

Figures 1a and 1b show XRCs of as-grown and annealed $In_{0.108}Ga_{0.892}As$ and $In_{0.108}Ga_{0.892}N_{0.017}As_{0.983}$ samples, respectively. The dashed lines correspond to simulation results. The $In_{0.108}Ga_{0.892}N_{0.017}As_{0.983}$ peak shifts closer to the GaAs substrate peak, demonstrating that adding N into $In_{0.108}Ga_{0.892}As$ layer does reduce the net compressive strain of the system. For N-containing samples, there are clear Pendelloesung fringes, indicating high crystalline quality and uniformity of the film, and the smooth interfaces between GaAs and InGaAsN. After RTA (700°C for 10s), the $In_{0.108}Ga_{0.892}As$ peak broadens, indicating strain relaxation. For $In_{0.108}Ga_{0.892}N_{0.017}As_{0.983}$, however, the Pendelloesung fringes after RTA at 700°C are sharper than those of the as-grown sample, indicating improved structural quality. After annealing at 850°C, the XRC peaks are still well resolved, indicating the $In_{0.108}Ga_{0.892}N_{0.017}As_{0.983}$ layer remains pseudomorphically strained and has better thermal stability than $In_{0.108}Ga_{0.892}As$ due to reduced lattice-mismatch (0.37 vs. 0.7%).

Secondary ion emission spectroscopy was performed on the samples to check the Be diffusion after RTA. It is found that no H is incorporated in $In_{0.108}Ga_{0.892}As$, but H is incorporated alongside N in as-grown InGaAsN samples, possibly due to the very large electronegativity of N atoms (N: 3.0, As: 1.57). The higher the N concentration is, the

more the H concentration. The free carrier concentration decreases with N incorporation mainly due to H passivation, which is also reported in MOCVD-grown InGaAsN samples. Figure 2 shows the SIMS profiles of as-grown (solid lines) and 700°C-annealed (dashed lines) for $In_{0.108}Ga_{0.892}N_{0.017}As_{0.983}$ samples. By annealing, H atoms dissociate from the $In_{0.108}Ga_{0.892}N_{0.017}As_{0.983}$ layer, so the H concentration is reduced. With increasing RTA temperature, the H concentration is further decreased, and the free carrier concentration increases. There is no detectable Be diffusion at 700°C RTA. At 850°C, some diffusion could be detected, and the free carrier concentration is also decreased.

Figure 3 shows the free carrier concentrations as a function of RTA temperature for as-grown and annealed InGaAsN samples. With the N concentration increasing from 0 to 0.024, the carrier concentration of the as-grown samples decreases by one order of magnitude, and the Hall mobility decreases from 60 to 30-45 cm^2/Vs. After RTA at 700°C, the carrier concentration of N-containing samples is increased to half that of GaInAs and the Hall mobility also increases to ~ 50 cm^2/Vs. Therefore, the product of carrier concentration and hole mobility is increased to half that of the GaInAs sample.

Several n-type InGaAsN layers were also grown[16], and the mobility is rather low, similar to MOCVD layers. For a carrier concentration of 10^{17} to 10^{18} cm^{-3} the room-temperature mobility is ~200 cm^2/Vs, which can be explained by the large electron effective mass and significant alloy scattering. Performing RTA shows that hydrogen atoms not only passivate the Si dopants but also act as n-type dopants. In summary, N incorporation in InGaAsN results in lower strain, better structural quality and thermal properties. Since here, hydrogen can come from cracked arsine, we now compare to MBE growth results using a solid As source.[17]

For InGaAsN samples grown by MBE using a solid As source, the SIMS measurements detected no H in these samples above the instrumental background of approximately 1×10^{18} cm^{-3}. Similarly, the concentration of C was below 1×10^{16} cm^{-3}. On the other hand, B was detected at levels between 5×10^{16} and 3×10^{17} cm^{-3}, depending on the N plasma source and power level used. This most likely results from sputtering of the boron nitride plasma chamber in the RF plasma source. In addition, a slight but significant increase in the level of O was detected for InGaAsN as compared to GaAs.

Unintentionally doped samples were p-type with room-temperature carrier concentrations of approximately 1×10^{16} cm^{-3}, and mobilities of approximately 200 cm^2/Vs. After annealing at 700°C for 15 minutes, the hole concentration increased slightly, to 2×10^{16} cm^{-3}, while the mobility remained essentially unchanged. N-type samples were also grown by doping with Si. Electron concentrations in these samples were factors of 10-20 lower than the estimated Si atomic concentrations of 5×10^{17} to 2×10^{18} cm^{-3}, and the mobilities were 200-300 cm^2/Vs. Upon annealing, the electron concentrations increased by a factor of two, and the mobilities increased slightly.

3. MINORITY CARRIER EFFECTS

To date, 1.0 eV bandgap InGaAsN has displayed promising minority carrier diffusion, required for solar cell operation, under very limited conditions. Under specialized growth and post –processing procedures, hole diffusion lengths as large as 0.6 to 0.8 μm have been observed in n-type, 1.0 eV InGaAsN, lattice matched to GaAs[7]. Negligible electron diffusion has been observed in p-type material. Further research is required to understand

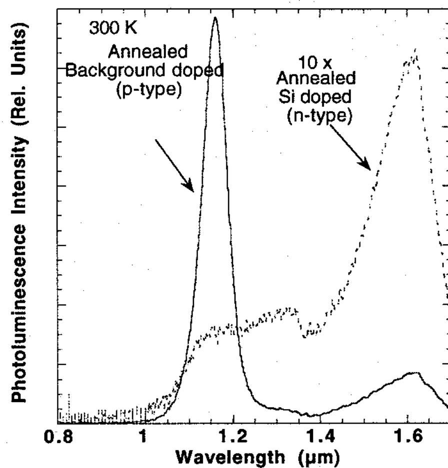

Figure 4. Photoluminescence spectra of n and p-type $In_{0.07}Ga_{0.93}As_{0.98}N_{0.02}$, after annealing.

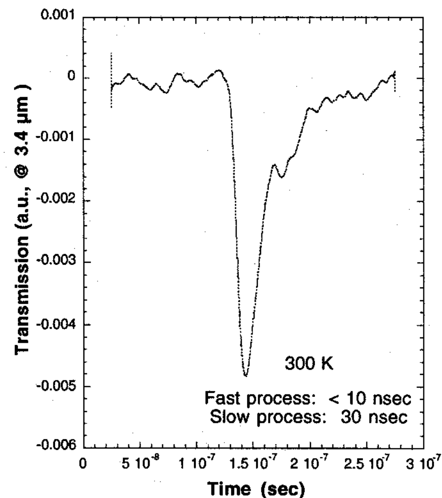

Figure 5. Time-resolved transmission of annealed p-type $In_{0.07}Ga_{0.93}As_{0.98}N_{0.02}$ at 3.4 µm, after pulsed excitation of electron-hole pairs.

those properties of InGaAsN which limit minority carrier diffusion and to identify material growth and processing conditions which produce viable material for solar cells.

Optical[7] and DLTS[15] studies show that InGaAsN (In=7%, N=2%) grown by MOCVD has several defects associated with doping and N incorporation. Photoluminescence spectra are shown in Fig. 4 for InGaAsN films grown under the same conditions and with nominally the same compositions as the n- and p-type regions of the solar cell. A band-edge photoluminescence peak was not observed in as-grown $In_{0.07}Ga_{0.93}As_{0.98}N_{0.02}$ films at 300K. After an ex-situ annealing process, a band-edge photoluminescence peak, approximately 60 meV linewidth, was observed in the p-type films. N-type doping with Si appears to introduce yet another defect or impurity into the InGaAsN.[15] With Si doping, the band-edge photoluminescence was weak both before and after ex-situ annealing (Fig. 4).

Consistent with photoluminescence results, initial studies indicate that carrier lifetime is longest for annealed, p-type $In_{0.07}Ga_{0.93}As_{0.98}N_{0.02}$ films. N-type or as-grown films had significantly shorter free carrier lifetimes. The carrier lifetime in annealed p-type material is controlled by a fast (< 10 nsec) process and a slower, temperature dependent, defect-moderated process (50 nsec @ 300K)and is shown in Fig. 5. This short lifetime (≈ 5 nsec) and typical Hall mobilities observed in our samples (≈ 200 cm^2/Vs) predict carrier diffusion lengths of ≈ 1 µm. Alloy scattering rates for electrons should be greater for XAsN or XSbN systems than other III-V alloys, and for InGaAsN, electron mobility is limited by alloy scattering. Alloy scattering is dependent upon spatial fluctuations in the chemical potential for the electrons or holes. These energy fluctuations are very large for GaAsN, and the fluctuations are proportional to the differences in electronegativity between the binary constituents (GaAs vs. GaN for example) or alternatively, the variation of conduction band energy with composition

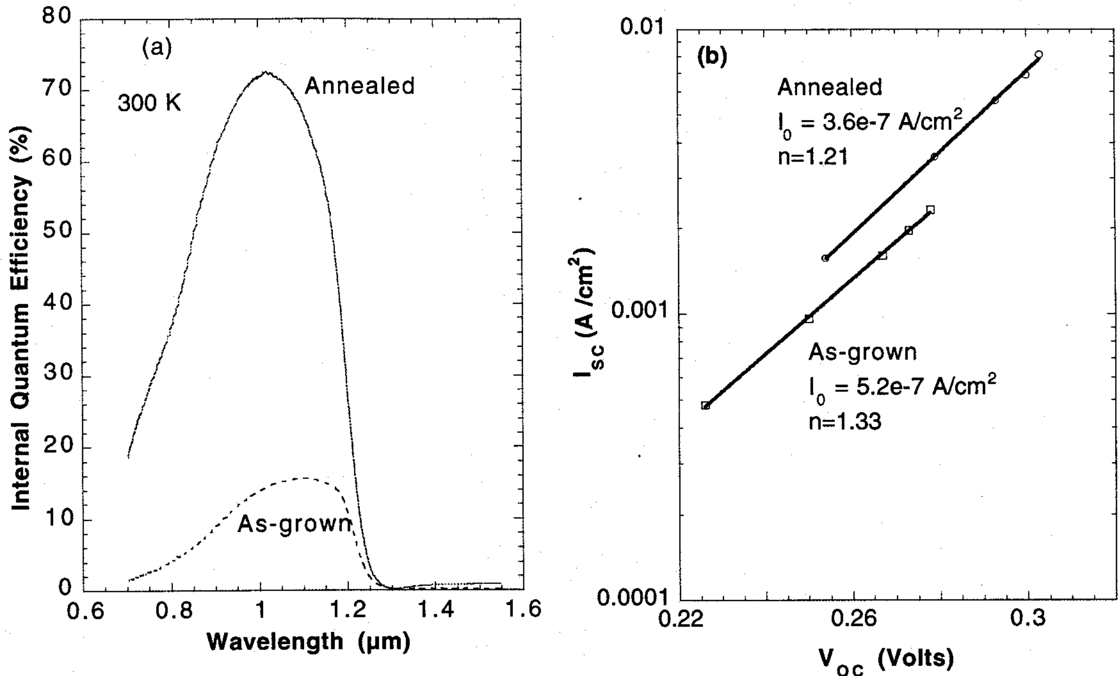

Figure 6. Internal quantum efficiencies of annealed and as-grown, 1.0 eV InGaAsN solar cells (Fig. 6 (a)) and short-circuit current (I_{sc}) and open-circuit voltage (V_{oc}) at different broadband light intensities for the cells in (Fig. 6 (a)) is shown in Fig. 6 (b)

Based on these annealing studies, a solar cell was constructed with a 1.0 μm thick, n-type (2×10^{17} cm^{-3}, Si doped) $In_{0.07}Ga_{0.93}As_{0.98}N_{0.02}$ emitter grown on a 1.0 μm thick, p-type (4×10^{16} cm^{-3}, background doped) base.[7] Internal quantum efficiency curves for both the annealed and as-grown cells are shown in Figure 6. The photoresponses extended out to the band-edge of the InGaAsN at 1.2 μm. Peak internal quantum efficiencies of > 70% were obtained for the annealed cell. Comparing the annealed and as-grown cells, annealing improved the quantum efficiency by roughly a factor of 5. Comparing the performance of a thick n-type emitter solar cell with thin n-type emitter cells and other alternative designs, it is found that negligible electron diffusion is occurring in the 1.0 eV p-type material (annealed or as-grown). To date, high quantum efficiencies have only been obtained with cell designs utilizing hole diffusion in n-type material.[7]

To estimate the minority carrier diffusion length in our cells, the photocurrent response versus bias was studied. Estimates show that the hole diffusion lengths are in the range of 0.6 to 0.8 μm (annealed) and 0.2 to 0.3 μm (as-grown). Despite the poor quality of the n-type material as indicated by optical studies, the improved efficiency of the annealed InGaAsN cell was due to diffusion of holes in the n-type emitter.[7] Electron diffusion lengths remain negligible (≈ 0.1 μm), leaving open the possibility that intrinsic, isovalent N sites produce electron localization in InGaAsN.

4. PHOTOMODULATION SPECTROSCOPY

Photomodulation spectroscopy has been used to measure the band gap energy of the $In_xGa_{1-x}N_yAs_{1-y}$ samples under hydrostatic pressure. The measurements were carried out

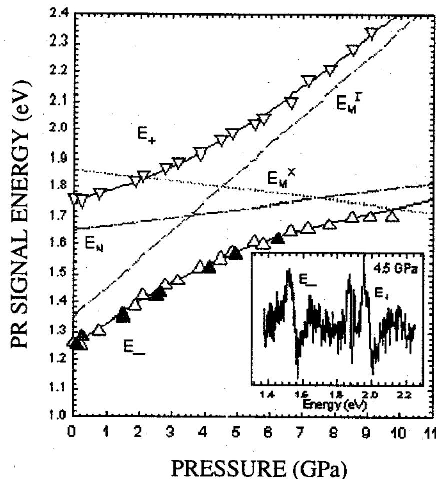

Figure 7. Change of the optical transition energies (E_- and E_+) in $In_{0.05}Ga_{0.95}N_{0.012}As_{0.988}$ as a function of applied pressure. The open triangles are experimental data. The solid lines are theoretical calculation results for the band anticrossing model. The dashed, dotted, and dot-dashed lines are the pressure dependence of the Γ and X conduction-band edges of the $In_{0.05}Ga_{0.95}As$ matrix and the N level relative to the top of the valence band, respectively. The inset shows a photoreflectance (PR) spectrum taken at 4.5 GPa. The narrow PR spectral feature at energy below E_+ is from the GaAs substrate.

in either transmission or reflection geometry at room temperature. Photomodulation spectroscopy is a differential method probing the variation of the absorptivity of the samples caused by the modulation of physical parameters such as the built-in surface field in the system.[18] The resulting spectra are characterized by features arising from direct interband transitions at high symmetry points in the band structure. Quasi-monochromatic light from a halogen tungsten lamp dispersed by a 0.5-m monochromator was focused on the samples as a probe beam. A chopped HeCd laser beam (4420Å) provided the photomodulation. The photo-modulated transmission signals were detected by either Ge or Si photodiode using a phase-sensitive lock-in amplification system. Application of pressure was accomplished by mounting small sample chips with sizes of ~200×200 mm^2 into gasketed diamond anvil cells.

It is found that in N containing material the fundamental gap or E_0 transition splits into two transitions E_- that represents the lowest energy gap and a higher energy E_+ transition. The splitting of the conduction band given by the energy difference $\Delta E = E_+ - E_-$ increases with increasing N content. Also, as is shown in Fig. 7, the energies of the E_+ and E- transitions show characteristic dependence on the hydrostatic pressure.[19] The observed effects find a simple and straightforward interpretation in terms of an anticrossing of a narrow band of localized N states and the extended states of the conduction band. The hydrostatic pressure changes the location of the N-level relative to the conduction band leading to an exemplary case of a level anticrossing behavior. The band anticrossing model explains very well the pressure dependence of the E_+ and E_- transitions. It also accounts for the pressure-induced change in the relative intensities of the photomodulation spectra for these transitions.[18]

The interaction between localized N-states and the conduction band leads also to a massive modification of the conduction band structure. Figure 8 shows the calculated dispersion relations for a parabolic conduction band interacting with dispersionless N-band. The conduction band splits into two highly non-parabolic subbands. The curvatures, and thus also the density of states effective masses strongly depend on the energy and the relative location of the nitrogen energy level E_N and the conduction band edge of the nitrogen-free host semiconductor matrix E_M. The predicted increase of the effective mass for the

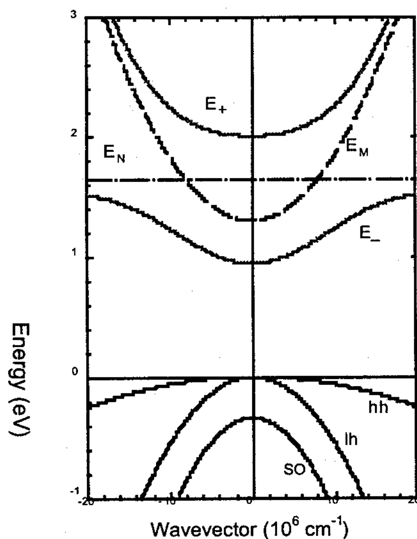

Figure 8. Calculated band structure showing anticrossing in the vicinity of the Γ point in the Brillouin zone for GaAsN. The dashed line represents the unperturbed curvature of the Γ conduction band of GaAs (E_M) and the dot-dashed line is the energy location of the highly localized N-state (E_N). The anticrossing interaction between the extended conduction-band states and a narrow band of the N resonant states results in a splitting of the conduction band into two nonparabolic subbands (E_- and E_+). The downward shift of the E_- subband edge is responsible for the reduction of the fundamental band-gap energy commonly observed in III-N-V alloys.

lower subband is consistent with recent magnetoluminescence measurements on InGaAsN quantum wells.[20]

The modifications of the conduction band structure have also profound effect on the transport properties of the conduction band electrons. It has been reported that the room temperature electron mobilities in InGaAsN alloys do not exceed 500 cm^2/Vs which is at least one order of magnitude lower than electron mobilities observed in N-free GaInAs alloys. This dramatic reduction of the electron mobilities can be explained by N-related alloy disorder scattering. In a simple approximation the strength of the alloy scattering can be related to the N-induced conduction band shift. In InGaAsN alloys this shift can be as large as 0.2 eV per atomic percent of N. This is at least an order of magnitude larger than typical band shifts observed in standard alloys. N-induced enhancement of the conduction band effective mass is another factor leading to the electron mobility reduction. Model calculations show that for GaNAs with 2% of N and electron concentration of 1×10^{17} cm^{-3} the mobility is reduced to 400 cm^2/Vs. This value is about 14 times smaller than the room temperature electron mobility in GaAs.[21]

The up-to-date research has demonstrated that group III-N-V alloys exhibit novel and quite extraordinary properties. However, future applications of these materials hinge on solving several outstanding issues associated with low electron mobilities and minority carrier lifetimes. Further research will be necessary to understand if the inferior material characteristics are intrinsic or extrinsic in nature. To these end systematic studies of factors affecting incorporation of lifetime limiting defects will be necessary. This will require a comprehensive approach that consists of a combination of materials synthesis and characterization techniques. Also more accurate calculations of the energy band structure and the effects of the modified conduction band on the electron mobility should be persuade to resolve the issue of intrinsic limitations of these materials. An important fundamental issue is the question whether III-N-V alloys is a unique system in which small change in

alloy composition produces such a large change in properties or if there exist other system that exhibit similar behavior.

5. BANDSTRUCTURE CALCULATIONS

Both first-principles[22-24] and empirical[25-28] theoretical treatments for this material system have concentrated on understanding the dependence of the bandgap energy on nitrogen composition. Recently, Jones et. al. have reported[29] the results of a first-principles electronic structure calculations based on the Kohn-Sham density functional theory with plane wave basis sets, ultrasoft pseudopotentials, and the local density approximation for the exchange-correlation functional. In construction of the pseudopotentials, the Ga 3d electrons were treated as valence electrons in order to accurately represent any effects of a near resonance with the nitrogen 2s level that has been observed in GaN.[30] The InGaAsN system in the experimentally relevant concentration range was modeled using a series of supercells of the zincblende GaAs structure each with a single arsenic replaced by a nitrogen. The lattice constants of the supercells were varied to simulate the effects of pressure, and for each cell, the ionic positions were relaxed using first-principles forces until the residual forces were less than 20 meV/Å. In all cases, it was found[29] that the nitrogen atom remained in the symmetric position during relaxation. In order to compare to experimental data, which is taken as a function of pressure, an *ab initio* calculation of the system pressure was performed. Several supercells were investigated with the following stoichiometries: $Ga_{32}As_{31}N$, $Ga_{64}As_{63}N$, $Ga_{108}As_{107}N$, and $Ga_{128}As_{127}N$. These cells correspond to nitrogen concentrations of 3.13, 1.56, 0.93 and 0.78%, with the nitrogen atoms ordered in simple cubic, fcc, bcc, and simple cubic lattices respectively. The calculated band structures of the various supercells were qualitatively similar despite their differing symmetries, indicating that the nitrogen atoms interact weakly with each other at these low concentrations leading to the conclusion that the artificially ordered supercells provide an adequate model of the near-band-gap electronic structure of the disordered experimental system.

Figure 9 shows a representative band structure for the 3.13% system. It should be noted that the band structure is plotted with respect to the Brillouin zone of a 64-atom cell. Since the nitrogen substitution breaks the symmetry of the underlying zincblende structure, there is no uniquely defined way to "unfold" the band structure into the Brillouin zone of the primitive 2-atom zincblende unit cell. The high symmetry points of the primitive GaAs cell fold into the Γ-point of the 64-atom cell, and therefore in the presence of a real symmetry breaking term (such as produced by nitrogen substitution), one expects interactions between the resulting levels. The valence band and the conduction band are indicated by the heavy solid line. The conduction band is well separated from the other bands throughout most of the Brillouin zone, and it is quite dispersive with a bandwidth more than 1 eV. Likewise, the bands above the conduction band show a substantial amount of dispersion, and there is no evidence of a flat impurity-like band near the conduction band energies shown in Fig. 9. The absence of a nitrogen derived impurity-like state is supported by a decomposition of the wave-functions in terms of atomic-like orbitals, which shows that the conduction band has about 5% of its weight on the nitrogen atom, which is by far the highest fraction of any of the bands above the gap.[22] The calculated bandgap is only 0.12 eV, while the experimental bandgap is of order 1 eV for this concentration of nitrogen. This large error in the bandgap is a well known problem of the LDA. A central result of this calculation is that despite this large error in the absolute magnitude of

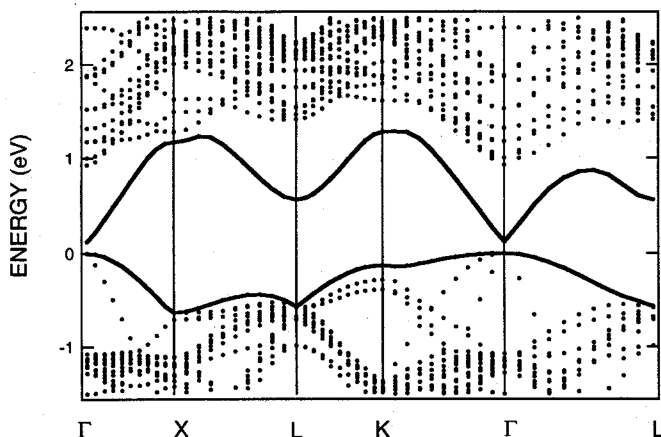

Figure 9. First principles local density approximation calculation for 3.3% nitrogen InGaAsN alloy. The solid lines, top and bottom, are respectively the conduction and valence bands.

the bandgap, the *change* in bandgap with lattice constant is in excellent agreement with experiment (see Fig.10).

A remarkable feature of Fig. 10 is the strongly non-linear dependence of the gap on the pressure. This is in marked contrast to the parent GaAs material and provides additional evidence, beyond the large reduction in the bandgap, that a few percent of nitrogen is producing remarkable changes in the material. In order to understand this nonlinearity, it is necessary to study additional bands above the conduction band. Figure 11 shows the theoretical pressure dependence of the Γ-point energies of several additional bands treated with the same analysis that was used for the conduction band in Fig. 10. Eight energy bands of the system are shown, but these fall into five degenerate groups. The figure shows three singlet states (filled circles), a doublet (open squares), and a triplet state (open triangles). Similar conclusions have also been recently reported by Mattila et. al.[31]

A common origin of nonlinear behavior of energy levels as a function of a parameter (such as pressure) is band repulsion. Band repulsion results from the mixing (hybridization) of bands in the same representation of the crystal symmetry group in such a way that level crossings are replaced with non-intersecting horizontal curves separated by a gap-like region. In Fig. 11, the highest singlet on the left and the triplet on the upper right bend downward due to repulsion from higher energy bands that have been omitted from the figure in order to improve its clarity.

With one exception, all of the bands within a few eV of the gap are observed to regain the degeneracies of pure GaAs to within of a few hundredths of an eV by the time the largest cell (0.78% N concentration) is reached. The exception is the L-derived singlet, which remains split off from the triplet by about 0.1 eV. This suggests that this singlet may evolve into the impurity state observed at very low nitrogen concentrations.[32,33] However, as mentioned above, this state does not act like an impurity state at the technologically interesting concentrations around 2%. Furthermore, the L-derived singlet rises faster than the conduction band throughout the studied pressure range, and we do not see the upward curvature that would be expected if it was repelled by the conduction band. Therefore, the conclusion is that repulsion between the L-derived singlet and the conduction band con-

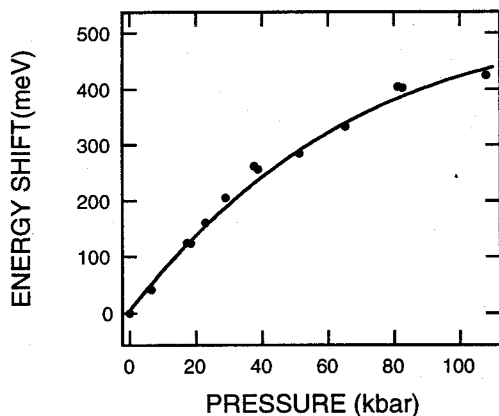

Figure 10. The pressure dependence of the 4-K bandgap energy shift, as determined from by the PL-peak energy, is shown as solid circles. The solid curve drawn through the data is a results of a first principles LDA band-structure calculation.[28]

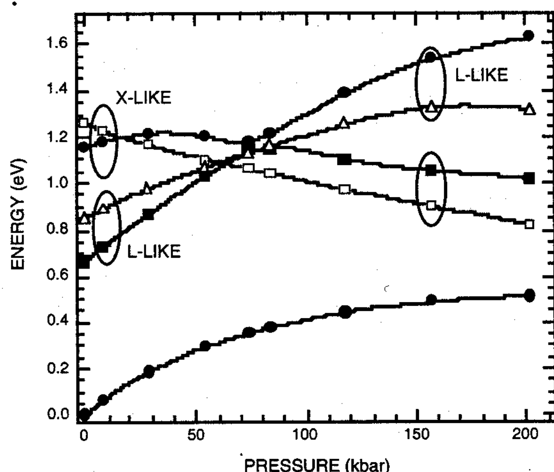

Figure 11. Theoretical pressure dependence of the conduction-band states near the bandgap energy minimum for 2% nitrogen GaAsN alloy. The points are calculated and there are three singlets (filled circles), a doublet (open squares), and a triplet state (open triangles).

tributes at most a small amount to the nonlinearity of the conduction band. In contrast, Fig. 11 demonstrates almost textbook repulsion between the X-derived singlet and the conduction band at pressures over 100 kbar, and it is likely that this repulsion continues to lower pressures, even though the effect is obscured by the additional repulsion between the X-derived singlet and a higher state. Based on these observations, the authors proposed[29] that repulsion from the X-derived singlet is the chief cause of the experimentally observed nonlinear dependence of the bandgap on pressure. Based on the above, these calculations lead to the conclusion that the nonlinear dependence of the bandgap on pressure does not result from localized nitrogen states.

6. ISSUES

InGaAsN Growth

The growth of InGaAsN alloys by MOCVD is difficult due to the unusual sensitivity of the alloy to growth conditions and the possible interaction between Group III and Group V sources. The growth rate depends on the total group III flux when the group V transport is fixed as is typical of III-V compound semiconductors. However, the growth rate has also been found to depend on the N/V ratio. Lower N/V ratios result in higher growth rates regardless of whether the AsH_3 flow is increased or the DMHy flux is decreased. Alloy composition in also very sensitive to growth temperature and the N/V gas phase ratio. The purity and chemical interaction of the nitrogen source (DMHy) now commonly used adds another uncertainty. Systematic investigation of how growth conditions

influence material properties such as background impurity incorporation, carrier trap density and energies and minority carrier properties should be pursued.

Localized vs. Delocalized States

Continued basic research on InGaAsN is required to address problems concerning the true picture going from localized electron states to a delocalized concept. Detailed transport studies in compensated InGaAsN are required to determine if electron localization is intrinsic to InGaAsN. More defect studies (optical spectroscopy, DLTS, resonant Raman, etc.) are needed understand the atomic nature of the N site and clusters. Defect studies will also be critical to improving electron and hole diffusion and guiding material growth.

However, future applications of these materials hinge on solving several outstanding issues associated with low electron mobilities and minority carrier lifetimes. Further research will be necessary to understand if the material characteristics are intrinsic or extrinsic in nature. To these end systematic studies of factors affecting incorporation of lifetime limiting defects will be necessary. This will require a comprehensive approach that consists of a combination of materials synthesis and characterization techniques. Also more accurate calculations of the energy band structure and the effects of the modified conduction band on the electron mobility should be persuade to resolve the issue of intrinsic limitations of these materials. An important fundamental issue is the question whether III-N-V alloys is a unique system in which small change in alloy composition produces such a large change in properties or if there exist other system that exhibit similar behavior.

Minority Carrier Lifetimes and Diffusion Lengths

Continued basic research on InGaAsN is required to address problems identified in these initial studies. Detailed transport studies in compensated InGaAsN are required to determine if electron localization is intrinsic to InGaAsN. More defect studies (optical spectroscopy, DLTS, resonant Raman, etc.) are needed understand the atomic nature of the N site and clusters. Defect studies will also be critical to improving electron and hole diffusion and guiding material growth. Concurrent studies of prototype solar cells will be critical optimize solar cell design to accommodate deficiencies of the InGaAsN material.

Solar Cell Design

The requirement that solar cells have good minority-carrier properties (i.e. long diffusion lengths / lifetimes) to achieve high efficiencies sets constraints on the materials systems that can be used for epitaxial growth of multilayer cell structures. A key constraint for the various epilayers in the structure regards their lattice constants compared to that of the substrate: since interface strain due to lattice mismatch generally lead to extended structural defects which adversely affect the minority-carrier properties of the layer. While schemes have been devised to control the propagation of such defects, a lattice-matched system is significantly easier to work with, and is the approach discussed here. Note that the structural properties of an epilayer affect the structure of all layers grown upon it; therefore, lattice-matching of the third junction in a three- or four-junction stack will affect the minority-carrier properties not only of the third junction itself, but also of the other two junctions grown on top of the third junction. Thus the condition or property that $Ga_{1-x}In_xN_yAs_{1-y}$ is lattice-matched to GaAs at x=3y is a key advantage of this alloy system. It should be noted, however, that lattice matching is not the only determinant of minority-carrier properties; as discussed below, the minority-carrier properties of (lattice-

matched) InGaAsN are the key challenges in making a useful solar cell from this alloy system.

For a cell serving as the third junction under InGaP and GaAs junctions, the efficiency of the device depends sensitively on the band gap of the third junction. Assuming an ideal device, as the band gap is raised above its optimal value of 1 eV, the amount of light available between its band gap and the band gap of the GaAs cell above it decreases, decreasing the photocurrent which the third junction is capable of producing. In the series-connected two-terminal configuration discussed here, once the photocurrent of the third junction is reduced below that of the InGaP/GaAs two-junction stack with which it is in series, the third junction will limit the photocurrent of the entire device, and will decrease rather than increase the overall device efficiency. On the other hand, as the band gap of the third junction is decreased below its 1 eV optimum (the 1 eV number assumes ideal device performance, in sharp contrast to the performance actually achieved for InGaAsN devices to date), the voltage of the third junction will decrease, reducing the efficiency boost provided by the third junction. Reducing the band gap of the third junction will also increase the photocurrent which the third junction is capable of producing; this may provide an approach to help meet the multijunction current-matching requirement for third junctions whose quantum efficiencies less than ideal. However, if a fourth junction is introduced below the three-junction InGaP/GaAs/InGaAsN structure for an additional efficiency boost, reducing the band gap of the third junction too far starts to steal too much light from the Ge fourth junction, once again reducing the overall multijunction device efficiency. The ability to control precisely the band gap of the third cell is therefore a requirement for the material used to fabricate it.

It should be emphasized that correctly measuring the IV curves for devices such as these, which are designed for operation under the spectral range of 1.0 to 1.4 eV, is not trivial. There are at least three causes for this difficulty: (1) the spectral range of 1-1.4 eV is very narrow, (2) the spectrum of the simulator's xenon lamp has multiple spikes in this spectral region, and (3) for terrestrial spectra, there are two large atmospheric-absorption notches in the 1.0-1.4 eV spectral range. Attempts to measure the current-voltage characteristics for these devices by using the conventional expedient of a reference cell are likely to result in significant errors if a xenon arc lamp is the light source.

Finally, concurrent studies of prototype solar cells will be critical optimize solar cell design to accommodate deficiencies of the InGaAsN material.

7. CONCLUSIONS

There has been considerable activity and progress during the 1998 to 1999 time period in obtaining new experimental data and thus allowing realistic theoretical modeling of the physical properties of the InGaAsN system. When all of the intrinsic properties are understood and extrinsic effects are identified, the real role or importance of InGaAsN as a candidate next generation thin film for photovoltaics material can be made.

8. ACKNOWLEDGEMENTS

The authors wish to thank Dr.'s R. M. Biefeld and A. Zunger for many valubale discussions and also for critical reading of the manuscript. Sandia is a multiprogram laboratory operated by Sandia Corporation, a Lockheed Martin Company, for the United States Department of Energy under contract DE-AC04-94AL85000. Part of this work was per-

formed at Lawrence Berkeley Laboratories, supported by the Director, Office of Energy Research, Office of Basic Energy Sciences, Division of Materials Sciences, of the US Department of Energy under contract No. DE-AC03-76SF00098. The work at the National Energy Renewable Laboratories was supported by the U.S. Department of Energy under Contract No. DE-AC36-98-GO10337. The work at UCSD is supported in part by a UC MICRO program with Rockwell International and the U.S.Army Research Office under the MURI "Low Power and Low Noise Electronics Technologies for Wireless Communications".

REFERENCES

1. W. G. Bi and C. W. Tu, Appl. Phys. Lett. **70**, 1608 (1997).
2. L. Malikova, F. H. Pollak, and R. Bhat, J. Electronic Materials **27**, 484 (1998).
3. M. Kondow, K. Uomi, A. Niwa, T. Kitatani, S. Watahiki, and Y. Yazawa, Jpn. J. Appl. Phys. **35**, 1273 (1996).
4. M. Kondow, T. Kitatani, S. Nakatsuka, M. C. Larson, K. Nakahara, Y. Yazawa, M. Okai, and K. Uomi, IEEE J. Selected Topics in Quantum Electronics **3**, 719 (1997).
5. T. Miyamoto, K. Takeuchi, F. Koyama, and K. Iga, IEEE Photonics Tech. Lett. **9**, 1448 (1997).
6. Sarah R. Kurtz, D. Myers, and J. M. Olsen, in *Proc. 26th IEEE Photovoltaics Spec. Conf.* (IEEE, New York, 1997) pp. 875-878.
7. Steven R. Kurtz, A. A. Allerman, E. D. Jones, J. M. Gee, J. J. Banas, and B. E. Hammons, Appl. Phys. Lett. **74**, 729 (1999).
8. E. V. K. Rao, A. Ougazzaden, Y. Le Bellego, and M. Juhel, Appl. Phys. Lett. **72**, 1409 (1998).
9. M. Weyers and M. Sato, Appl. Phys. Lett. **62**, p. 1396 (1993).
10. S. Miyoshi et al, J. Crystal Growth **124**, 439 (1992).
11. A. Ougazzaden, Appl. Phys. Lett. **70**, 2861 (1997).
12. D. J. Friedman, J. F. Geisz, S. R. Kurtz, J. M. Olson, R. Reedy, J. Crystal Growth, **195**, 438 (1998).
13. J.F. Geisz, J. Crystal Growth **195**, 401 (1998).
14. S. Kurtz, Appl. Phys. Lett., **74**, 729 (1999).
15. D. Kwon, R. J. Kaplar, S. A. Ringel. A. A. Allerman, S. R. Kurtz, and E. D. Jones, Appl. Phys. Lett.**74**, 2830 (1999).
16. C. Tu (Private Communication).
17. J. F. Klem (Unpublished Results).
18. M. Cardona, in *Modulation Spectroscopy*, (Academic Press, New York, 1969)
19. W. Shan, W. Walukiewicz, J. W. Ager III, E. E. Haller, J. F. Geisz, D. J. Friedman, J. M. Olson and Sarah R. Kurtz, Phys. Rev. Lett. **82**, 1221 (1999).
20. E. D. Jones, N. A. Modine, A. A. Allerman, I. J. Fritz, S. R. Kurtz, A. F. Wright, S. T. Tozer, and X. Wei, in *Light-Emitting Diodes: Research, Manufacturing, and Applications III,* edited by E. F. Schubert, I. T. Ferguson, and H. W. Yao, SPIE Conference Proceedings Vol. **3621** (International Society for Optical Engineering, Bellingham, WA, 1999), pp. 52-63.
21. W. Walukiewicz, J. Lagowski, L. Jastrzebski, M. Lichtensteiger and H. C. Gatos, J. Appl. Phys. **50**, 899 (1979)
22. A. Rubio and M. L. Cohen, Phys. Rev. B **51**, 4343(1995).
23. J. Neugebauer and C. G. Van de Walle, Phys. Rev. B **51**, 10568 (1995).
24. S.-H. Wei and A. Zunger, Phys. Rev. Lett. **76**, 664 (1996).
25. L. Bellaiche, S.-H. Wei, and A. Zunger, Phys. Rev. B **54**, 17568 (1996).

26. L. Bellaiche, S.-H. Wei, and A. Zunger, Appl. Phys. Lett. **70**, 3558 (1997).
27. L. Bellaiche, S.-H. Wei, and A. Zunger, Phys. Rev. B **56**, 10233 (1997).
28. L. Bellaiche and A. Zunger, Phys. Rev. B **57**, 4425 (1998).
29. E. D. Jones, N. A. Modine, A. A. Allerman, S. R. Kurtz, A.F. Wright, S. T. Tozer, and X. Wei, to be published, Phys. Rev. B (July 15 1999).
30. V. Fiorentini, M. Methfessel, and M. Scheffler, Phys. Rev. B **47**, 13353 (1993).
31. T. Mattila, S-H. Wei, and A. Zunger, to be published Phys Rev B.
32. D. J. Wolford, J. A. Bradley, K. Fry, and J. Thompson, in *Physics of Semiconductors*, ed. J. D. Chadi and W. A. Harrison (Springer, New York, 1984) pp. 627-630.
33. X. Liu, M. E. Pistol, L. Samuelson, S. Schwetlick, and W. Seifert, Appl. Phys. Lett. **56**, 1451 (1990).